Overexpression of CuZn superoxide dismutase protects RAW 264.7 macrophages against nitric oxide cytotoxicity

Florian BROCKHAUS and Bernhard BRÜNE[1]

University of Erlangen-Nürnberg, Faculty of Medicine, Department of Medicine IV, Loschgestrasse 8, 91054 Erlangen, Germany

Initiation of nitric oxide ($NO^{\bullet}$)-mediated apoptotic cell death in RAW 264.7 macrophages is associated with up-regulation of mitochondrial manganese superoxide dismutase (MnSOD; SOD2) and down-regulation of cytosolic copper zinc superoxide dismutase (CuZnSOD; SOD1) at their individual mRNA and protein levels. To evaluate the decreased CuZnSOD expression and the initiation of apoptosis we stably transfected macrophages to overexpress human CuZnSOD. Individual clones revealed a 2-fold increase in CuZnSOD activity. Expression of a functional and thus protective CuZnSOD was verified by attenuated superoxide ($O_2^{\bullet-}$)-mediated apoptotic as well as necrotic cell death. In this study we showed that SOD-overexpressing macrophages (R-SOD1-12) were also protected against $NO^{\bullet}$-initiated programmed cell death. Protection was substantial towards $NO^{\bullet}$ derived from exogenously added NO donors or when $NO^{\bullet}$ was generated by inducible NO synthase activation, and was evident at the level of p53 accumulation, caspase activation and DNA fragmentation. Stimulation of parent and SOD-overexpressing cells with a combination of lipopolysaccharide and murine interferon γ produced equivalent amounts of nitrite/nitrate, which ruled out attenuated inducible $NO^{\bullet}$ synthase activity during protection. Because protection by a $O_2^{\bullet-}$-scavenging system during $NO^{\bullet}$-intoxication implies a role of $NO^{\bullet}$ and $O_2^{\bullet-}$ in the progression of cell damage, we used uric acid to delineate the role of peroxynitrite during $NO^{\bullet}$-elicited apoptosis. The peroxynitrite scavenger uric acid left *S*-nitrosoglutathione or spermine-NO-elicited apoptosis unaltered, blocking only 3-morpholinosydnonimine-mediated cell death. As a result we exclude peroxynitrite from contributing, to any major extent, to $NO^{\bullet}$-mediated apoptosis. Therefore protection observed with CuZnSOD overexpression is unlikely to stem from interference with peroxynitrite formation and/or action. Unequivocally, the down-regulation of CuZnSOD is associated with $NO^{\bullet}$ cytotoxicity, whereas CuZnSOD overexpression protects macrophages from apoptosis.

Key words: apoptosis, caspases, glutathione, Mn superoxide dismutase, p53.

INTRODUCTION

Nitric oxide ($NO^{\bullet}$), an important pleiotropic molecule, shapes various physiological and pathophysiological conditions, and participates in immune regulation, neurotransmission and host defence [1]. Under circumstances of excessive generation such as various pathological or inflammatory conditions, $NO^{\bullet}$ mediates microbial and tumour cell killing and is regarded a destructive agent towards cells and tissue. $NO^{\bullet}$ is synthesized from the guanidino nitrogen of L-arginine by constitutive and inducible isoforms of nitric oxide synthase (NOS; EC 1.14.13.39) in response to various agonists [2]. Several cell types such as activated macrophages produce not only $NO^{\bullet}$ but also superoxide ($O_2^{\bullet-}$), which, in a diffusion-controlled way, reacts with $NO^{\bullet}$ to form peroxynitrite ($ONOO^-$) [3]. The cytotoxicity of $NO^{\bullet}$, $ONOO^-$ or various NO_x oxidation products might stem from the interaction with iron–sulphur proteins, transition metals or protein thiols, or might occur as a result of damage to DNA [4].

Cytotoxicity evoked by the massive formation of radicals, i.e. $NO^{\bullet}$ or $O_2^{\bullet-}$, can be ascribed to apoptosis or necrosis, two defined features of the cell death programme [5]. Apoptosis is an essential programme for maintaining homoeostasis in multicellular organisms [6]. Morphological and biochemical apoptotic features comprise chromatin condensation, DNA fragmentation, cell shrinkage and dissolution of the cell into apoptotic bodies [7]. Initiation of the death programme is achieved by a wide variety of stimuli, with the identification of gene products that positively or negatively modulate the progression of the cell suicide pathway [8]. Accumulation of the tumour suppressor protein p53 is an early marker of $NO^{\bullet}$-elicited apoptosis in macrophages that seems to be closely linked to the death programme, as p53-anti-sense expression largely attenuated macrophage death [9]. The executive phase of apoptosis is characterized by catalytically active cysteine proteases, known as caspases. Caspases are inactive proenzymes that are processed proteolytically to their active multimeric forms [10,11] to cleave multiple proteins in a sequence following an aspartic residue. So far at least ten distinctive family members have been grouped by substrate specificity and their role as initiators or executors of the death pathway [12]. In contrast with apoptosis, necrosis is regarded as accidental cell death [13], with characteristic signs of cell swelling, membrane rupture, randomly digested DNA and cell dissolution [7].

Cells have elaborated protective mechanisms to cope with potentially damaging molecules such as reactive oxygen species by synthesizing antioxidant enzymes [14]. Superoxide dismutases (SODs) are key cellular defence systems that disproportionate $O_2^{\bullet-}$ into oxygen and H_2O_2, with the latter being detoxified by glutathione peroxidase or catalase. Eukaryotic cells contain two types of SOD: CuZnSOD (also known as SOD1) and MnSOD (also referred to as SOD2) [15]. CuZnSOD is located in the cytosol, is expressed constitutively and is considered a housekeeping enzyme. The down-regulation of CuZnSOD by anti-sense oligonucleotides allows cell death in PC12 cells in response

Abbreviations used: DMNQ, 2,3-dimethoxy-1,4-naphthoquinone; GSNO, *S*-nitrosoglutathione; IFN-γ, murine interferon γ; L-NAME, N^G-nitro-L-arginine methyl ester; LDH, lactate dehydrogenase; LPS, lipopolysaccharide; MnTMPyD, Mn(III)tetrakis(1-methyl-4-pyridyl)porphyrin; $NO^{\bullet}$, nitric oxide; NOS, nitric oxide synthase; $O_2^{\bullet-}$, superoxide; $ONOO^-$, peroxynitrite; SIN-1, 3-morpholinosydnonimine; SOD, superoxide dismutase.

[1] To whom correspondence should be addressed (e-mail mfm423@rzmail.uni-erlangen.de).

to withdrawal of trophic factors or the generation of oxidative stress [16], whereas the transfection of CuZnSOD into mouse L-cells or human HeLa cells attenuates paraquat (i.e. $O_2^{\bullet-}$-mediated) toxicity [17,18]. In contrast, MnSOD is located in mitochondria. The expression of MnSOD is subject to intense modulation by various stimuli, including cytokines, bacterial lipopolysaccharide (LPS) [19] or NO$^\bullet$ [20].

In the present study we examined the role of SOD during NO$^\bullet$-mediated apoptosis in RAW 264.7 macrophages. We specifically followed the expression of CuZnSOD and MnSOD in response to NO$^\bullet$ and examined apoptotic parameters in macrophages that had been engineered to overexpress CuZnSOD stably. We conclude that the enforced expression of CuZnSOD attenuates NO$^\bullet$-mediated apoptosis, and discuss potential protective mechanisms.

EXPERIMENTAL

Materials

Spermine-NO was purchased from Research Biotrend (Cologne, Germany). Diphenylamine and sheep secondary antibody were from Sigma (Deisenhofen, Germany). DEVD-AMC was from Biomol (Hamburg, Germany). Mouse and rabbit secondary antibodies came from Promega/Serva (Heidelberg, Germany). Anti-(human CuZnSOD) was from Calbiochem (Bad Soden, Germany). Anti-(rat CuZnSOD) and anti-(rat MnSOD) antibodies were kindly provided by Professor K. Asayama (Yamanashi Medical University, Yamanashi, Japan). Hybridoma supernatant against p53, clone Pab122, was used with the kind permission of Professor H. Stahl (Universität des Saarlandes, Homburg/Saar, Germany). The human CuZnSOD recombinant expression plasmid (p·GSOD-SVneo) was kindly provided by Professor Y. Groner (Weizmann Institute of Sciene, Rehovot, Israel). PCR primers for mouse CuZnSOD, MnSOD and glyceraldehyde-3-phosphate dehydrogenase were obtained from Eurogentec (Seraing, Belgium). Moloney-murine-leukaemia virus reverse transcriptase, $(dT)_{12-18}$, *Taq* DNA polymerase, cell-culture supplements and fetal-calf serum were purchased from Gibco (Berlin, Germany). RPMI 1640 was from Biochrom (Berlin, Germany). All other chemicals were of the highest grade of purity commercially available.

Cell culture

Mouse RAW 264.7 and R-SOD1-12 cells were maintained in RPMI 1640 supplemented with 100 i.u./ml penicillin, 100 μg/ml streptomycin and 10 % (v/v) heat-inactivated fetal-calf serum (complete RPMI). All experiments were performed with complete RPMI. For nitrite/nitrate determinations, cells were cultured in high-glucose Dulbecco's modified Eagle's medium supplemented as described for RPMI 1640.

Transfection of RAW 264.7 cells

Mouse RAW 264.7 cells (2×10^6 cells) were stably transfected with 20 μg of a human CuZnSOD expression vector (p·GSOD-SVneo) carrying the human CuZnSOD gene under a SV40 promoter and a *neo* transcriptional unit by using the calcium phosphate precipitation method [21]. Selection was started 48 h after transfection with the antibiotic G418 (500 μg/ml). Stably transfected single clones were isolated by using the limiting dilution method, were propagated in complete RPMI 1640/G418, and then examined for the expression of human CuZnSOD.

Determination of SOD activity

CuZnSOD activity was determined by following the inhibition of nitrite formation from hydroxylammonium chloride in the presence of $O_2^{\bullet-}$ generators by using the method of Elstner and Heupel [22]. In brief, cells were permeabilized with 0.5 % (v/v) Nonidet P40. Protein was measured by using the DC Protein Assay (Bio-Rad Laboratories, München, Germany). The reaction mixture (0.2 ml) contained a SOD standard or cell extract (25 μg) in 65 mM phosphate buffer (pH 7.8)/7.5 mM xanthine/5 mM hydroxylammonium chloride/0.05 unit/ml xanthine oxidase (EC 1.1.3.22) in the presence or absence of 0.5 mM KCN. Samples were incubated at 25 °C for 20 min. Nitrite formation was determined by adding 50 μl of 10 μM sulphanilic acid/1 μM α-naphthylamine to an equal volume of sample. The absorbance was determined at 530 nm.

One unit of SOD activity was defined as the amount of purified SOD (EC 1.15.1.1) producing 50 % inhibition of nitrite formation under standard conditions by blotting nitrite generation at increasing concentrations of SOD. The unknown SOD activity of samples was calculated and expressed in units per mg of protein. Differentiation between MnSOD and CuZnSOD was performed by the addition of 0.5 mM KCN. CuZnSOD activities were defined as those inhibited by KCN. The difference between total SOD activity and KCN-attenuated enzyme activity was defined as MnSOD activity.

Synthesis of *S*-nitrosoglutathione (GSNO)

GSNO was synthesized as described previously [23]. In brief, GSH was dissolved in 0.625 M HCl at 4 °C to a final concentration of 625 mM. An equimolar quantity of $NaNO_2$ was added and the mixture was stirred for 40 min. After the addition of acetone the precipitate was collected, washed and dried under vacuum. Freshly synthesized GSNO was characterized by UV spectroscopy.

Quantification of DNA fragmentation

DNA fragmentation was assayed as reported [24]. In brief, after incubations, cells (2.5×10^6) were centrifuged, resuspended in 250 μl of TE buffer [10 mM Tris/HCl (pH 8.0)/1 mM EDTA], and lysed for 30 min at 4 °C by adding 250 μl of cold lysis buffer containing 2 mM EDTA, 0.5 % (v/v) Triton X-100 and 5 mM Tris/HCl, pH 8.0. Centrifugation (15 min at 14000 ***g***) separated intact chromatin (pellet) from DNA fragments (supernatant). Pellets were resuspended in 500 μl of TE buffer; DNA was precipitated by adding 500 μl of 10 % (w/v) trichloroacetic acid at 4 °C. Samples were pelleted at 4000 ***g*** for 10 min and the supernatant was removed. After the addition of 300 μl of 5 % (w/v) trichloroacetic acid, samples were boiled for 15 min. The DNA contents of pellets and supernatants were measured separately by using the diphenylamine reagent. The percentage of fragmented DNA was calculated as the ratio of the DNA content in the supernatant to the amount in the pellet.

Quantification of apoptotic cells

Cells (4×10^5) were grown in 12-well plates. Cells were stimulated, followed by fixation on glass slides with 3 % (w/v) paraformaldehyde for 5 min. Samples were washed with PBS, stained with Hoechst dye H33258 (1.5 μg/ml) for 5 min, washed with distilled water and mounted in Kaiser's glycerol gelatin. Nuclei were

revealed with a Zeiss fluorescence microscope (Axiovert 100). In each sample a minimum of 200 cells were counted and apoptotic nuclei were expressed as the percentage of total nuclei.

Release of lactate dehydrogenase (LDH)

The percentage of LDH release was expressed as the proportion of LDH released into medium as compared with the total amount of LDH present in the cells as determined by lysis of cells with 0.1 % (v/v) Triton X-100. LDH activity was monitored as the oxidation of NADH by following the decrease in A_{334}. Reactions were performed in 50 mM triethanolamine buffer, pH 7.6, containing 5 mM EDTA, 127 mM pyruvate and 14 mM NADH.

Determination of fluorogenic caspase-3 activity

Cells (4×10^6) were incubated as indicated, recovered from cultured plates and centrifuged (1200 ***g***, 4 °C, 5 min). Cell pellets were resuspended in lysis buffer [100 mM Hepes (pH 7.5)/10 % (w/v) sucrose/0.1 % (v/v) CHAPS/1 mM PMSF/10 μg/ml pepstatin/10 μg/ml leupeptin/1 mM EDTA] and left on ice for 30 min. After sonification (Branson sonifier, 10 s, duty cycle 100 %, output control 1), lysates were centrifuged (10000 ***g***, 10 min, 4 °C) and protein content was determined with the DC protein assay. Cell supernatants (30 μg of protein) were incubated in 100 mM Hepes (pH 7.5)/10 % (w/v) sucrose/0.1 % (v/v) CHAPS/1 mM EDTA/1 mM PMSF/10 μg/ml leupeptin at 30 °C with 12 μM of the caspase-3 substrate DEVD-AMC. Substrate cleavage was followed fluorimetrically with excitation at 360 nm and emission at 460 nm during a 90 min incubation.

Reverse transcriptase-mediated PCR

Total RNA was isolated by acid guanidinium thiocyanate/phenol/chloroform extraction [25]. Total RNA (1 μg) was converted into cDNA by incubation in 50 mM Tris/HCl, pH 8.3, containing 1 μM $(dT)_{12-18}$, dNTPs (0.5 mM each), 75 mM KCl, 3 mM $MgCl_2$, 10 mM dithiothreitol, 1 unit/μl RNase inhibitor, and 10 units/μl Moloney-murine-leukaemia virus reverse transcriptase at 37 °C for 1 h. Amplification of CuZnSOD and MnSOD was performed by incubating 10 ng equivalents of DNA in 20 mM Tris/HCl, pH 8.4, containing 50 mM KCl, 1.5 mM $MgCl_2$, dNTPs (200 μM each) and 0.05 unit/μl *Taq* DNA polymerase with the following oligonucleotide primers: for detection of CuZnSOD, 5′-GGATCCATGGCGATGAAAGCGGTGTGC-3′ and 5′-AAGCTTGGGAATGTTTACTGCGCAATCCCA-3′; for detection of MnSOD, 5′-ATGTTGTGTCGGGCGGCG-3′ and 5′-AGGTAGTAAGCGTGCTCCCACACG-3′. The sequence of glyceraldehyde-3-phosphate dehydrogenase was amplified as a control under identical conditions with the primers 5′-CCATCAACGACCCCTTCATTGACC-3′ and 5′-GAAGGCCATGCCAGTGAGCTTCC-3′. PCR was performed with 25 cycles of 30 s at 96 °C, 30 s at 60 °C and 1 min at 72 °C. PCR products were analysed on 1.5 % (w/v) agarose gels.

Western blots of CuZnSOD, MnSOD and p53

After CuZnSOD, MnSOD and p53 had been expressed they were analysed by Western blotting. In brief, 3×10^6 cells were incubated for the times indicated, followed by cell lysis in 200 μl of 50 mM Tris/HCl (pH 8.0)/5 mM EDTA/150 mM NaCl/0.5 % (v/v) Nonidet P40/1 mM PMSF. Cells were sonicated with a Branson sonifier (10 s, duty cycle 100 %, output control 1). After centrifugation (14000 ***g***, 15 min) supernatants were analysed for protein content. Protein (25 μg for the detection of CuZnSOD and MnSOD, or 150 μg for the detection of p53) was mixed with the same volume of 2 × sample buffer [125 mM Tris/HCl (pH 6.9)/2 % (w/v) SDS/10 % (v/v) glycerol/1 mM dithiothreitol/0.002 % Bromophenol Blue] and boiled for 10 min. Proteins were resolved by SDS/PAGE [15 % (CuZnSOD and MnSOD) or 10 % (p53) gel], and blotted on nitrocellulose sheets. Molecular masses were determined in relation to a rainbow molecular mass marker. Transblots were washed twice with TBS [140 mM NaCl/50 mM Tris/HCl (pH 7.2)] containing 0.1 % (v/v) Tween 20 before non-specific binding was blocked with TBS/5 % (v/v) skimmed milk. First antibodies against human CuZnSOD, mouse CuZnSOD and mouse MnSOD were dissolved in TBS/0.5 % (v/v) milk and used at a dilution of 1:750, 1:20000 and 1:20000 respectively. The p53 antiserum was diluted 1:5. Antibodies were incubated overnight at 4 °C. Blots were washed five times and non-specific binding was blocked as described above. For final detection, blots were incubated with horseradish peroxidase-conjugated anti-sheep, anti-rabbit or anti-mouse immunoglobulins [1:10000 in TBS/0.5 % (v/v) milk] for 1 h, followed by detection by enhanced chemiluminescence.

Nitrite/nitrate determination

Nitrite, a stable product of NO• oxidation, was determined by the Griess reaction. Culture supernatants (200 μl) were collected, mixed with 20 μl of sulphanilamide (dissolved in 1.2 M HCl) and 20 μl *N*-naphthylethylenediamine dihydrochloride. After 5 min at room temperature, A_{560} was measured against a reference wavelength at 690 nm. Nitrite concentrations were calculated by using a $NaNO_2$ standard. Total NO• production was determined by analysing both nitrite and nitrate by using a standard method [26]. In brief, the assay uses two steps: first, the enzymic reduction of nitrate to nitrite with nitrate reductase (EC 1.6.6.2), FAD and NADPH; secondly, derivatization and spectrophotometric detection of nitrite as described above after interfering NADPH has been removed enzymically.

Determination of GSH

After incubations, RAW 264.7 and R-SOD1-12 cells were scraped off, centrifuged and washed twice with PBS. Cells were lysed by the addition of 300 μl of 1 % (w/v) sulphosalicylic acid for at least 10 min at 4 °C before centrifugation (12000 ***g***, 5 min). The GSH content in the supernatant (40 μl) was measured by the method of Tietze et al. [27], which is based on the reaction of GSH with 5,5′-dithiobis-(2-nitrobenzoic acid) (150 μM). Intra-assay signal amplification was achieved by reducing GSSG back to GSH with glutathione reductase (8 μg/ml) and NADPH (0.2 mM), dissolved in buffer A [0.1 M potassium phosphate/1 mM EDTA (pH 7.5)]. The rate of formation of 5-thio-2-nitrobenzoate was measured at 405 nm for 2 min and GSH concentrations were calculated by using a GSH standard.

Statistical analysis

Each experiment was performed at least three times and statistical analysis was performed with the two-tailed Student's *t* test. A normal distribution of data was ensured. SOD activities are expressed as means ± S.E.M. for at least three determinations. Otherwise, representative results, of at least three similar examinations, are shown.

RESULTS

Expression of CuZnSOD and MnSOD in response to NO•

In a first set of experiments we examined CuZnSOD and MnSOD expression at the mRNA and protein level in RAW 264.7 macrophages after their exposure to NO• donors such as GSNO and spermine-NO. Macrophages were incubated for 3–8 h with 500 μM GSNO or 250 μM spermine-NO (Figure 1). Basal expression of CuZnSOD at the mRNA and protein level was down-regulated by NO• (Figures 1A and 1B). Decreased mRNA expression was evident at 3 h and became more pronounced at 6 h. Protein expression was slightly decreased at 4 h in response to GSNO and spermine-NO and was drastically decreased at 8 h (Figures 1A and 1B, left panels).

In contrast, MnSOD behaved differently. mRNA levels were time-dependently up-regulated in response to GSNO. This was noticed after 3 and 6 h (Figure 1A, right panels). Increased mRNA levels resulted in elevated protein expression that started at 4 h and was clearly visible at 8 h (Figure 1B, right panels). In addition, functional activities of CuZnSOD and MnSOD were determined in RAW 264.7 cells treated for 8 h with 500 μM GSNO. Residual CuZnSOD activity (25.9 $\pm$ 2.1 units/mg of protein) was decreased by NO• (20.7 $\pm$ 0.7 units/mg of protein), whereas MnSOD activity was elevated from control values (1.5 $\pm$ 0.8 units/mg of protein) by NO• (7.2 $\pm$ 2.8 units/mg of protein). As established here (see Figure 3) and in previous examinations, the addition of 500 μM GSNO or 250 μM spermine-NO promoted apoptosis in RAW 264.7 macrophages [28].

We next examined SOD expression in response to endogenously produced NO•. Macrophages were activated with 1 μg/ml LPS in combination with 10 i.u/ml murine interferon γ (IFN-γ) for 15 h (Figures 1C and 1D). The expression of CuZnSOD and MnSOD varied again. CuZnSOD was down-regulated at the mRNA and protein level in response to LPS/IFN-γ (Figures 1C and 1D, left panels). Decreased expression was partly reversed by blocking endogenous NO• generation with N^G-nitro-L-arginine methyl ester (L-NAME), a NOS inhibitor. This was more pronounced at the mRNA level as compared with protein

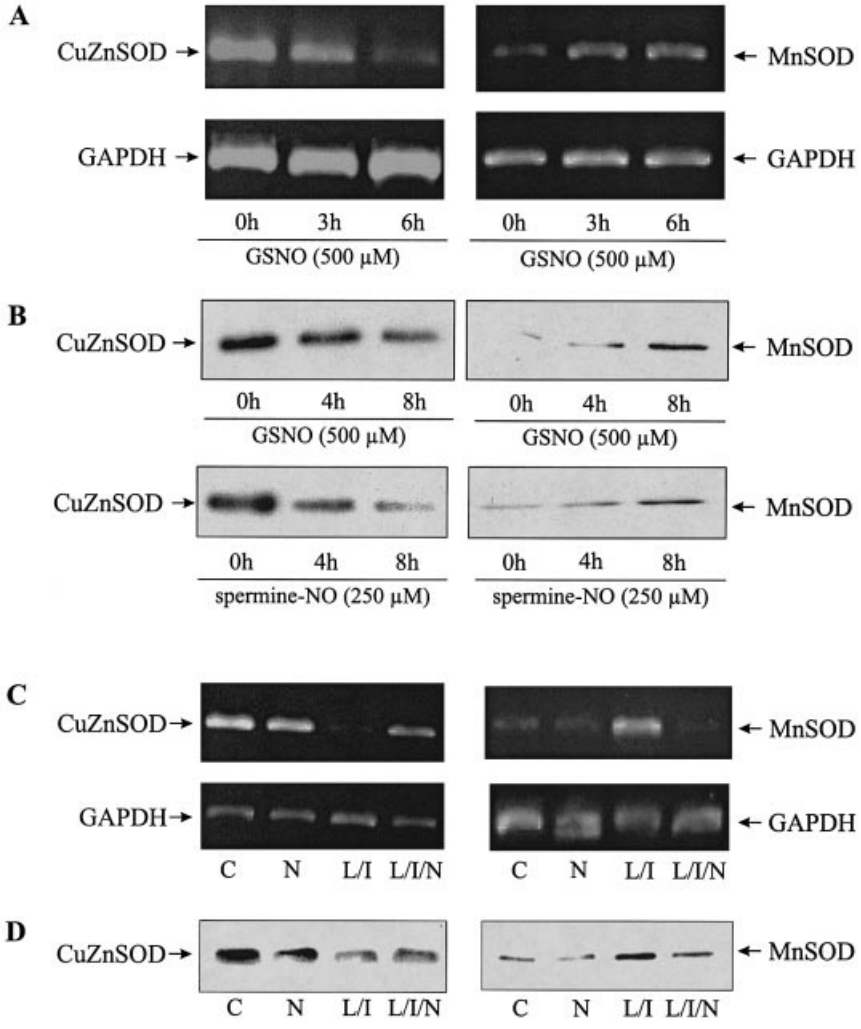

Figure 1 Expression of CuZnSOD and MnSOD in response to NO•

RAW 264.7 cells were incubated with 500 μM GSNO and 250 μM spermine-NO for the durations indicated. mRNA expression (**A**) and protein levels (**B**) of CuZnSOD and MnSOD were determined. Alternatively, mRNA (**C**) and protein expression (**D**) were analysed in response to 1 μg/ml LPS and 10 i.u./ml IFN-γ, or to combinations of LPS, IFN-γ and L-NAME (C, control; N, L-NAME; L, LPS; I, IFN-γ), incubated for 15 h. CuZnSOD and MnSOD expression were examined by reverse transcriptase-mediated PCR and Western-blot analysis as described in the Experimental section. Each Figure is representative of three independent experiments.

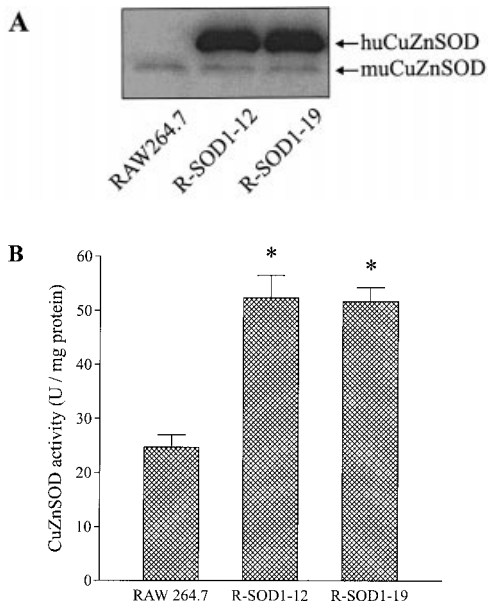

Figure 2 CuZnSOD overexpression in RAW 264.7 cells

(**A**) RAW 264.7 cells and two CuZnSOD transfectants (R-SOD1-12 and R-SOD1-19) were examined for expression of human CuZnSOD (huCuZnSOD) and mouse CuZnSOD (muCuZnSOD) proteins by Western-blot analysis as described in the Experimental section. (**B**) CuZnSOD specific activity was determined as described in the Experimental section. Results are representative of three similar experiments. $^*P < 0.05$ compared with RAW 264.7 cells.

Table 1 DMNQ-mediated fragmentation of DNA and release of LDH

RAW 264.7 and R-SOD1-12 cells (2×10^6 cells per assay) were exposed for 24 h to 5 or 10 μM DMNQ. DNA fragmentation and LDH release were quantified as outlined in the Experimental section. Results are means $\pm$ S.E.M. for at least four separate experiments. $^*P < 0.05$ compared with individual controls.

	DNA fragmentation (%)		LDH release (%)	
[DMNQ] (μM)	RAW 264.7	R-SOD1-12	RAW 264.7	R-SOD1-12
0 (control)	1.32 $\pm$ 0.58	2.41 $\pm$ 1.61	7.68 $\pm$ 3.27	6.80 $\pm$ 1.63
5	11.41 $\pm$ 4.93*	2.07 $\pm$ 1.00	33.29 $\pm$ 2.56*	5.98 $\pm$ 1.60
10	18.12 $\pm$ 1.59*	7.92 $\pm$ 5.02	48.08 $\pm$ 7.34*	14.05 $\pm$ 5.62

expression. L-NAME itself left CuZnSOD expression unaltered. In contrast, mRNA and protein expression of MnSOD were up-regulated by LPS/IFN-γ (Figures 1C and 1D, right panels). Increased MnSOD expression was completely attenuated by L-NAME and was therefore NO$^\bullet$-mediated. Consistently with these alterations at the mRNA and protein levels, LPS/IFN-γ decreased CuZnSOD activity from 26.9 $\pm$ 4.6 to 17.7 $\pm$ 2.2 units/mg of protein and increased MnSOD activity from 2.7 $\pm$ 0.8 to 10.1 $\pm$ 3.9 units/mg of protein. Activities of CuZnSOD and MnSOD remained basically at control levels (CuZnSOD, 23.4 $\pm$ 3.6 units/mg of protein; MnSOD, 2.9 $\pm$ 0.7 units/mg of protein) when cells were treated with the combination of LPS/IFN-γ and L-NAME. NO$^\bullet$ production in response to LPS/IFN-γ and suppression of NOS activity by L-NAME was verified by nitrite determination in the cell supernatant by the Griess method. LPS/IFN-γ significantly increased nitrite values (1.98 $\pm$ 0.67 μM in controls compared with 18.35 $\pm$ 2.46 μM with LPS/IFN-γ), whereas L-NAME in combination with LPS/IFN-γ decreased nitrite levels to those in controls (5.24 $\pm$ 1.76 μM). In this (see Figure 4) and previous examinations we established that endogenous NO$^\bullet$ formation initiated apoptosis, whereas L-NAME attenuated the activation of the cell death pathway [29]. Collectively our results imply that NO$^\bullet$ up-regulated the expression of MnSOD, whereas in contrast CuZnSOD was down-regulated. As NO$^\bullet$ under these conditions promoted apoptosis we sought to overexpress CuZnSOD and thereby modulate cell death pathways.

Overexpression of active CuZnSOD in RAW 264.7 macrophages

RAW 264.7 macrophages were stably transfected with human CuZnSOD-encoding plasmids. Figure 2(A) shows the overexpression of human CuZnSOD in two selected cell clones, named R-SOD1-12 and R-SOD1-19, as compared with mock-transfected macrophages (RAW 264.7). The lower protein band recognized by the antibody represents the basal expression of mouse CuZnSOD.

Activity determinations of CuZnSOD confirmed the overexpression of a functional enzyme (Figure 2B). Cell clones overexpressing CuZnSOD revealed a 2-fold higher specific activity than controls.

With the use of the redox cycler and $O_2^{\bullet-}$-generating agent 2,3-dimethoxy-1,4-naphthoquinone (DMNQ) we established protection of the CuZnSOD-overexpressing clone R-SOD1-12 as compared with parent cells (Table 1). Exposure of RAW 264.7 cells to 5 or 10 μM DMNQ resulted in apoptosis as quantified by the diphenylamine assay, and cell necrosis as determined by LDH release.

In CuZnSOD-overexpressing clones apoptotic and/or necrotic cell death parameters were absent. These results underscore the fact that CuZnSOD-overexpressing cells are endowed with the capacity to detoxify high levels of $O_2^{\bullet-}$ and to prevent the initiation of apoptotic or necrotic cell-destructive pathways.

CuZnSOD overexpression and NO$^\bullet$-mediated apoptosis

We next investigated whether the expression of CuZnSOD also affected NO$^\bullet$-mediated cytotoxicity. RAW 264.7 cells and R-SOD1-12 cells were exposed to 500 μM GSNO or 250 μM spermine-NO, before the assessment of DNA fragmentation, caspase-3 activity and p53 accumulation (Figure 3). GSNO and spermine-NO caused DNA fragmentation in RAW 264.7 cells within 8 h, whereas internucleosomal DNA cleavage was substantially attenuated in R-SOD1-12 clones (Figure 3A). Decreased DNA fragmentation seen in R-SOD1-12 cells was not compensated for by increased LDH release (results not shown).

Because the activation of caspases is an inherent feature of apoptotic cell death, we examined the cleavage of the fluorogenic caspase-3 substrate DEVD-AMC in parent and SOD-overexpressing cells (Figure 3B). GSNO (500 μM) or spermine-NO (250 μM) promoted significant caspase-3 activation within 5 h, which resulted in the accumulation of aminomethylcoumarin as a consequence of DEVD-AMC proteolysis. However, NO$^\bullet$ donors only marginally activated caspase-3 in R-SOD1-12 cells.

In corroboration of earlier examinations, we observed the accumulation of tumour suppressor p53 in response to NO$^\bullet$ formation, i.e. GSNO (500 μM) addition. As p53 accumulation is an early marker of NO$^\bullet$-mediated apoptotic cell death we performed a Western-blot analysis after a 4 h incubation period with GSNO (Figure 3C). p53 accumulation seen in parent macrophages was absent from SOD-overexpressing cells. These examinations revealed an attenuated apoptotic response after the addition of NO$^\bullet$ donors in cells that overexpress CuZnSOD.

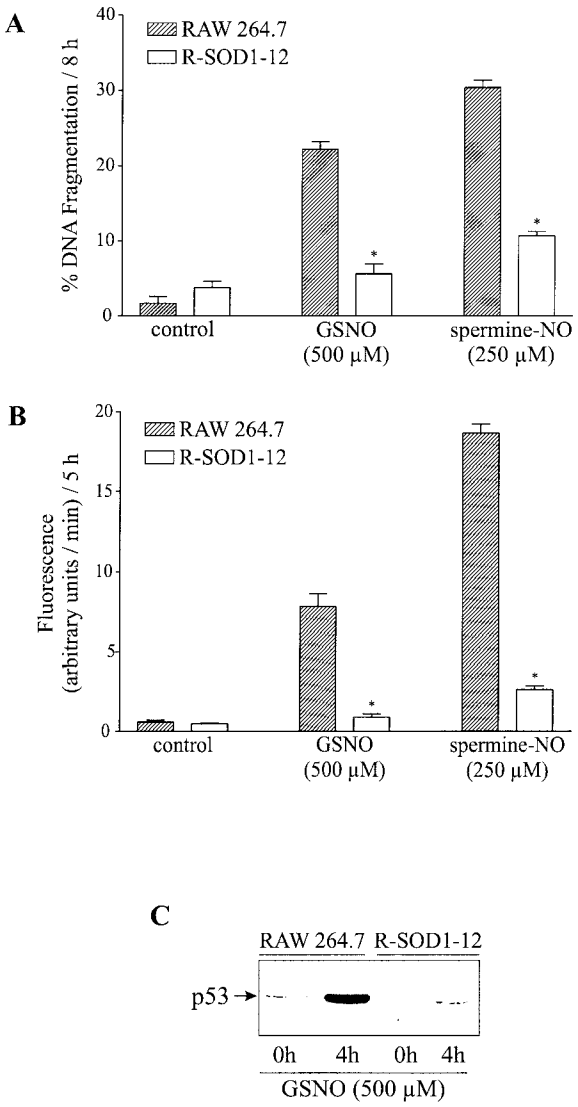

Figure 3 CuZnSOD overexpression attenuates NO• donor-mediated apoptosis

(**A**) RAW 264.7 cells or R-SOD1-12 cells were incubated with 500 μM GSNO or 250 μM spermine-NO. DNA fragmentation was quantified after 8 h by using the diphenylamine assay. (**B**) Caspase-3 activity was determined after 5 h by the cleavage of the fluorogenic caspase-3 substrate DEVD-AMC. (**C**) Accumulation of p53 was measured after 4 h by Western blot analysis. For details see the Experimental section. Results are means $\pm$ S.E.M. for at least four separate experiments. *$P < 0.001$ compared with GSNO and with spermine-NO-treated RAW 264.7 cells.

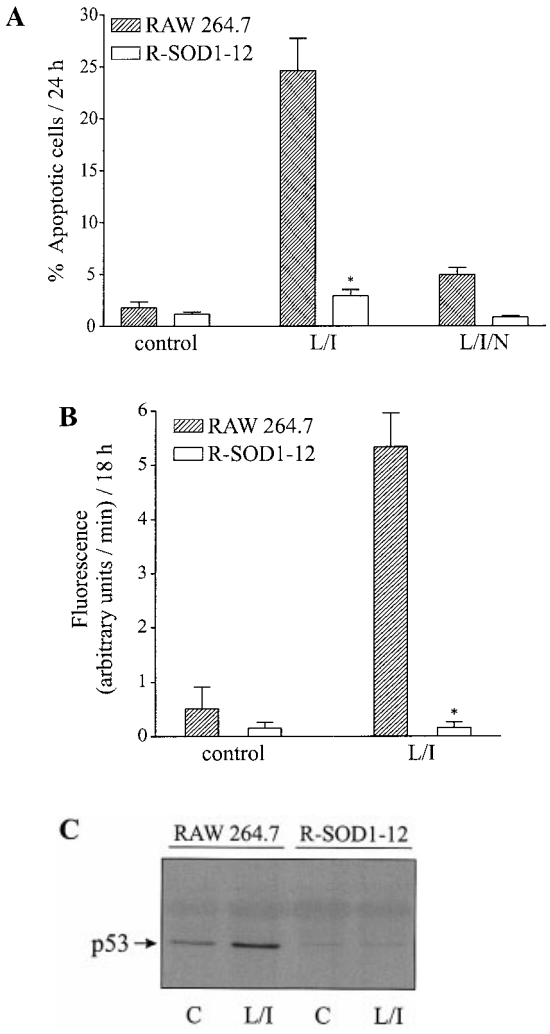

Figure 4 CuZnSOD overexpression abrogates apoptosis after the induction of inducible NOS

RAW 264.7 and R-SOD1-12 cells were incubated with LPS (L; 1 μg/ml), IFN-γ (I; 10 i.u./ml) or both agonists in the absence or presence of 1 mM L-NAME (N; 1 mM). (**A**) Apoptotic cells were scored after incubations with the DNA-specific fluorochrome Hoechst dye 33258, 24 h after stimulation. (**B**) Caspase-3 activity was determined 18 h after stimulation by measuring cleavage of the fluorogenic substrate DEVD-AMC. (**C**) The accumulation of p53 was detected by Western-blot analysis 16 h after stimulation. For details see the Experimental section. Results are means $\pm$ S.E.M. for at least four separate experiments. *$P < 0.001$ compared with L-NAME/IFN-γ-treated RAW 264.7 cells.

Further experiments elucidated the apoptotic response in parent and SOD-transfected cells after the formation of endogenous NO• (Figure 4). When RAW 264.7 macrophages were challenged with 1 μg/ml LPS in combination with 10 i.u./ml IFN-γ for 24 h, we noticed approx. 25 % apoptotic cells in parent cultures by scoring chromatin condensation in affected cells. Apoptosis was NO•-mediated, because L-NAME brought fragmentation values back to those in controls (Figure 4A). On stimulation of R-SOD1-12 cells we observed no fragmentation. An examination of LDH activity ruled out necrosis under these experimental conditions.

An analysis of caspase-3 activation revealed the same picture. In LPS/IFN-γ-stimulated RAW 264.7 cells we measured caspase-3 activity, whereas caspase activation in SOD-overexpressing cells was absent (Figure 4B). Supporting evidence for attenuated apoptosis in stably SOD-transfected cells came from p53 analysis performed 16 h after stimulation with LPS/IFN-γ (Figure 4C). p53 accumulation was noticed in parent but not in R-SOD1-12 cells.

Collectively our results point to an inhibition of NO•-mediated apoptosis in CuZnSOD-transfected cells. To rule out the possibility that sustained apoptosis in SOD-overexpressing cells simply resulted from attenuated NO• generation, we analysed nitrite and nitrate values after cell activation (Table 2). RAW macrophages activated with a combination of 1 μg/ml LPS and 10 i.u./ml IFN-γ for 16 h responded with nitrite and nitrate accumulation in the cell supernatant, thus indicating NO• forma-

Table 2 Nitrite and nitrate levels in RAW 264.7 and R-SOD1-12 macrophages

RAW 264.7 and R-SOD1-12 cells (4×10^5 cells per assay) were exposed for 16 h to 1 μg/ml LPS and 10 i.u./ml IFN-γ (LPS/IFN-γ), LPS/IFN-γ in the presence of 1 mM L-NAME (LPS/IFN-γ/L-NAME) or L-NAME alone, or remained as controls. Nitrite/nitrate was determined by the Griess reaction as described in the Experimental section. Results are means $\pm$ S.E.M. for four separate experiments. $^*P < 0.001$ compared with individual controls.

	RAW 264.7		R-SOD1-12	
Treatment	[Nitrite] (μM)	[Nitrate] (μM)	[Nitrite] (μM)	[Nitrate] (μM)
Control	2.23 $\pm$ 0.21	7.17 $\pm$ 1.83	0.03 $\pm$ 0.01	9.59 $\pm$ 0.61
L-NAME	1.17 $\pm$ 0.85	9.40 $\pm$ 1.17	0.02 $\pm$ 0.01	8.16 $\pm$ 0.92
LPS/IFN-γ	21.43 $\pm$ 1.21*	31.25 $\pm$ 3.17*	22.46 $\pm$ 3.16*	33.62 $\pm$ 5.20*
LPS/IFN-γ/L-NAME	6.56 $\pm$ 1.42	14.26 $\pm$ 2.34	4.12 $\pm$ 1.01	12.78 $\pm$ 1.32

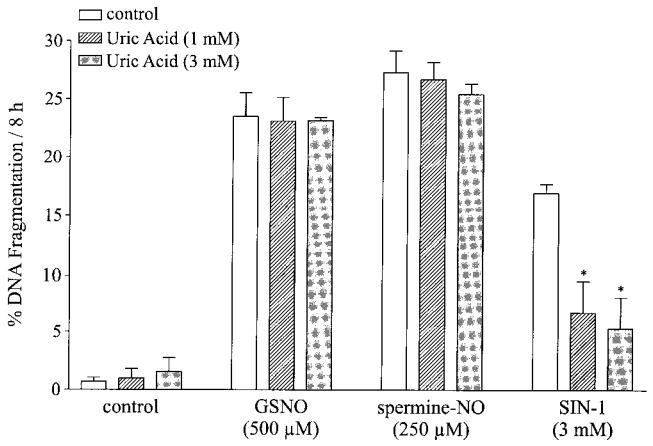

Figure 5 NO$^\bullet$ donor-induced fragmentation of DNA in the presence of uric acid

RAW 264.7 cells were exposed for 8 h to 500 μM GSNO, 250 μM spermine-NO or 3 mM SIN-1, or remained as controls. Uric acid (1 or 3 mM) was added 1 h before agonist. DNA fragmentation was quantified by using the diphenylamine assay as described in the Experimental section. Results are means $\pm$ S.E.M. for three individual experiments. $^*P < 0.05$ compared with SIN-1-treated RAW 264.7 cells.

tion. The nitrite and nitrate levels were approximately equal, and L-NAME substantially decreased the generation of NO$^\bullet$.

The response of R-SOD1-12 cells was equivalent. Nitrite and nitrate accumulation was noticed after LPS/IFN-γ addition; moreover it was L-NAME-sensitive. We observed no statistical difference between parent and SOD-transfected cells. Thus we can exclude decreased NO$^\bullet$ generation as a likely explanation for the inhibition of apoptosis in SOD-overexpressing cells.

Potential role of ONOO$^-$ and GSH

Protection from NO$^\bullet$-elicited apoptosis in CuZnSOD-overexpressing cells points to a likely involvement of $O_2^{\bullet-}$ and/or the participation of ONOO$^-$, which is produced by the NO$^\bullet$/$O_2^{\bullet-}$ interaction. To elucidate any potential cytotoxic role of ONOO$^-$ we made use of uric acid, an effective ONOO$^-$ scavenger (Figure 5). RAW 264.7 macrophages were preincubated with 1 or 3 mM uric acid, followed by the addition of 500 μM GSNO, 250 μM spermine-NO or 3 mM of the ONOO$^-$ generating compound 3-morpholinosydnonimine (SIN-1). After an 8 h incubation period we analysed for internucleosomal DNA fragmentation.

The ONOO$^-$ scavenger uric acid left the response to GSNO and spermine-NO unaltered but significantly decreased SIN-1-mediated apoptosis. In extension, the ONOO$^-$ scavenger ebselen at concentrations ranging from 10 to 50 μM showed no interference during NO$^\bullet$-evoked apoptosis (results not shown). On the basis of the above-mentioned experiments we excluded any significant contribution of ONOO$^-$ during NO$^\bullet$-elicited apoptosis. Taking into consideration the fact that variations in the intracellular redox potential, i.e. GSH, affect apoptotic signal-transducing pathways in Bcl-2- and Hsp27-overexpressing cells we analysed for GSH in parent and stably SOD-transfected cells. We found that the GSH content in R-SOD1-12 cells was 39.7 $\pm$ 4.2% higher than in RAW 264.7 cells. These elevated levels of GSH might contribute to protection of R-SOD1-12 cells against NO$^\bullet$-mediated cytotoxicity.

DISCUSSION

The present study demonstrates that gene transfer resulting in enforced expression of the antioxidant enzyme CuZnSOD attenuates apoptotic cell death in macrophages. Overexpression of CuZnSOD not only protected macrophages against $O_2^{\bullet-}$-mediated apoptosis but also abrogated NO$^\bullet$-initiated programmed cell death, as characterized by DNA fragmentation, caspase activation and p53 accumulation.

We realized that, under conditions of NO$^\bullet$-elicited apoptosis, the expression and functional activities of SOD isoenzymes are subjected to regulation. Whereas MnSOD became activated and expressed at a higher rate, CuZnSOD was down-regulated at the mRNA, protein and activity levels. It has been noticed that antisense-evoked down-regulation of CuZnSOD in PC12 cells permitted apoptosis in response to different NO$^\bullet$ donors [16]. Antisense-enforced SOD down-regulation and our observations that NO$^\bullet$ simultaneously decreased CuZnSOD expression and promoted apoptosis in RAW 264.7 cells led to the assumption that both events are correlated. To test this hypothesis, we stably transfected RAW 264.7 macrophages with a human CuZnSOD-encoding plasmid. CuZnSOD-overexpressing RAW 264.7 cells (R-SOD1-12 and R-SOD1-19) showed an approximate doubling in CuZnSOD activity and were protected against $O_2^{\bullet-}$-mediated apoptosis. As expected, SOD-overexpressing cells cope with higher levels of oxygen radicals generated by redox-cycling agents, thereby preventing the initiation of apoptotic signalling pathways. Our findings are in line with reports showing that CuZnSOD-overexpressing cells are resistant against paraquat-mediated toxicity [17] or that CuZnSOD-deficient fetal fibroblasts are more sensitive than wild-type cells to paraquat [18]. Overexpression of SOD in association with only a doubling in activity is in line with previous reports [30,31] and can be rationalized by a self-protective mechanism, because higher expression of SOD might result in toxicity [17]. Moreover these results imply that mitochondrial MnSOD is unable to substitute for cytosolic CuZnSOD activity [32].

As revealed by our investigation, the overexpression of CuZnSOD not only protects against oxygen-radical-mediated toxicity but also abrogates NO$^\bullet$-elicited programmed cell death. Parameters that characterize NO$^\bullet$-initiated apoptosis, such as p53 accumulation, caspase activation or DNA fragmentation, are absent from SOD-transfected cells. Control examinations excluded decreased NO$^\bullet$ formation as the underlying protective principle and substantiated the possibility that enforced SOD expression does not alter the nitrite-to-nitrate ratio in response to stimulation with LPS/IFN-γ. One might conclude that a direct

reaction between NO• and SOD that redirects NO• metabolism is unlikely to occur under cellular conditions and makes this possibility a less favourable explanation for protection. Interestingly, this is in contrast with the enforced expression of MnSOD, which interferes in NO• metabolism by attenuating the up-regulation of inducible NOS, thereby lowering nitrite/nitrate values [33].

Of course, protection in association with a doubling in specific CuZnSOD activity raises the question of whether NO•-mediated apoptosis demands oxygen-radical formation that promotes cell death, either directly or indirectly, via the formation of $ONOO^-$. This assumption seems to be supported by the observation of decreased neurotoxicity with the addition of SOD in response to *S*-nitrosocysteine, by showing attenuated cell death in the gut after the addition of SOD and *S*-nitroso-*N*-acetyl-DL-penicillamine [34,35], or by establishing that SOD mimetics attenuate the NO•-mediated inhibition of mitochondrial respiration [36]. However, several discrepancies of our study in comparison with the mentioned reports preclude any simple unifying explanation. SOD mimetics such as Mn(III)tetrakis(1-methyl-4-pyridyl)porphyrin (MnTMPyD) have been shown to interfere at multiple sites with the NO• system or the action of NO• donors. MnTMPyD directly scavenges NO• or interferes with NOS and/or soluble guanylate cyclase and therefore cannot be considered as a specific SOD mimetic [37]. Other studies employed rather high concentrations of SOD to observe protection and therefore cannot exclude side effects such as the direct interaction of NO• with SOD [38]. Although NO• is implicated in the inhibition of the mitochondrial respiratory chain [39] and $ONOO^-$ is known to inactivate MnSOD [40], both of which promote higher $O_2^{\bullet -}$ levels, an argument that favours the contribution of oxygen radicals during RAW macrophage cell death is not easily supported. If one assumes $O_2^{\bullet -}$ formation, which would allow $ONOO^-$ generation on the addition of NO•, one should predict protection by using the $ONOO^-$ scavenger uric acid, which enters cells and/or mitochondria to detoxify endogenously produced $ONOO^-$ [41,42]. From our study it seems that NO•-donor-elicited apoptosis remains unaltered even in the presence of high concentrations of the $ONOO^-$ scavengers uric acid or ebselen, thus making any contribution of the $NO^\bullet/O_2^{\bullet -}$ interaction product under our experimental conditions unlikely. However, we noticed protection by uric acid when a $ONOO^-$-generating agent, SIN-1, initiated apoptosis. It is therefore unlikely that the protection afforded by SOD stems from interference with oxygen radical formation and/or reaction. Further examinations will elucidate whether the increase in GSH is relevant for protection. On the basis of the observations that Bcl-2 [43] or Hsp27 [44] overexpression protects cells in part by promoting an increase in GSH and further taking into account that *N*-acetylcysteine abrogated NO•-initiated apoptosis [45], an alteration in the amount of GSH will attract our close consideration and direct further studies.

NO• is known to affect gene regulation, which in our study is exemplified by the regulation of SOD [46]. Up-regulation of MnSOD is found in association with the endogenous or exogenous production of NO• and is in accordance with earlier studies showing an increased mRNA expression of MnSOD in NO•-stimulated macrophages [20]. An increased expression of MnSOD is also noticed in apoptotic human macrophages exposed to oxidized low-density lipoprotein, tumour necrosis factor α or H_2O_2. Anti-sense oligonucleotides directed against MnSOD caused an inhibition of protein expression and decreased apoptosis [47]. In macrophages the expression of MnSOD is obviously correlated with apoptosis, which is underscored by our finding that NO• initiated apoptosis and MnSOD expression. Further studies need to address the signalling pathway that promotes MnSOD up-regulation at the mRNA and protein levels. Interestingly, CuZnSOD is down-regulated in association with NO•-evoked apoptosis. Decreased protein expression as a result of massive generation of NO• is reported for several proteins such as adhesion molecules or cytokines and is in part rationalized by the inhibition of transcription factors such as nuclear factor-κB, activating protein-1 or Egr-1. Recently it was shown that mitomycin inhibits CuZnSOD gene transcription through p53-mediated transcriptional repression [48]. Molecular details on sustained CuZnSOD expression and the potential role of p53 in association with the onset of apoptosis await further clarification.

Decreased CuZnSOD expression under conditions of NO•-elicited apoptosis and protection from cell death by enforced CuZnSOD expression suggest a critical role of CuZnSOD in macrophage transducing pathways that promote apoptosis.

This work was supported by the Deutsche Forschungsgemeinschaft, the European Community and the Deutsche Krebshilfe.

REFERENCES

1 Schmidt, H. H. and Walter, U. (1994) Cell **78**, 919–925
2 Nathan, C. (1992) FASEB J. **6**, 3051–3064
3 Crow, J. and Beckman, J. S. (1995) Adv. Pharmacol. **34**, 17–43
4 Brüne, B., von Knethen, A. and Sandau, K. B. (1998) Eur. J. Pharmacol. **351**, 261–272
5 MacMicking, J., Xie, Q. W. and Nathan, C. (1997) Annu. Rev. Immunol. **15**, 323–350
6 Vaux, D. L. and Strasser, A. (1996) Proc. Natl. Acad. Sci. U.S.A. **93**, 2239–2244
7 Wyllie, A. H., Kerr, J. F. and Currie, A. R. (1980) Int. Rev. Cytol. **68**, 251–306
8 Schwartzman, R. A. and Cidlowski, J. A. (1993) Endocr. Rev. **14**, 133–151
9 Messmer, U. K. and Brüne, B. (1996) Biochem. J. **319**, 299–305
10 Patel, T., Gores, G. J. and Kaufmann, S. H. (1996) FASEB J. **10**, 587–597
11 Zhivotovsky, B., Burgess, D. H., Vanags, D. M. and Orrenius, S. (1997) Biochem. Biophys. Res. Commun. **230**, 481–488
12 Cohen, G. M. (1997) Biochem. J. **326**, 1–16
13 Walker, N. I., Harmon, B. V., Gobé, G. C. and Kerr, J. F. R. (1988) Methods Achiev. Exp. Pathol. **13**, 18–54
14 Sies, H. (1993) Eur. J. Biochem. **215**, 213–219
15 Fridovich, I. (1995) Annu. Rev. Biochem. **64**, 97–112
16 Troy, C. M., Derossi, D., Prochiantz, A., Greene, L. A. and Shelanski, M. L. (1996) J. Neurosci. **16**, 253–261
17 Elroy-Stein, O., Bernstein, Y. and Groner, Y. (1986) EMBO J. **5**, 615–622
18 Huang, T. T., Carlson, E. J., Leadon, S. A. and Epstein, C. J. (1992) FASEB J. **6**, 903–910
19 Visner, G. A., Dougall, W. C., Wilson, J. M., Burr, I. A. and Nick, H. S. (1990) J. Biol. Chem. **265**, 2856–2864
20 Sano, H., Hirai, M., Saito, H., Nakashima, I. and Isobe, K. I. (1997) Immunology **92**, 118–122
21 Weisz, A., Ciccatiello, L. and Esumi, H. (1996) Biochem. J. **316**, 209–215
22 Elstner, E. F. and Heupel, A. (1976) Anal. Biochem. **70**, 616–620
23 Hart, T. W. (1985) Tetrahedron Lett. **26**, 2013–2016
24 McConkey, D. J., Nicotera, P., Hartzell, P., Bellomo, G., Wyllie, A. H. and Orrenius, S. (1989) Arch. Biochem. Biophys. **269**, 365–370
25 Chomczynski, P. and Sacchi, N. (1987) Anal. Biochem. **162**, 156–159
26 Schmidt, H. H. H. and Kelm, M. (1996) in Methods in Nitric Oxide Research (Feelisch, M. and Stamler, J. S., eds.), pp. 491–497, John Wiley, New York
27 Tietze, F. (1969) Anal. Biochem. **27**, 502–522
28 Messmer, U. K. and Brüne, B. (1996) Arch. Biochem. Biophys. **327**, 1–10
29 Messmer, U. K., Lapetina, E. G. and Brüne, B. (1995) Mol. Pharmacol. **47**, 757–765
30 Teixeira, H. D., Schumacher, R. I. and Meneghini, R. (1998) Proc. Natl. Acad. Sci. U.S.A. **95**, 7872–7875
31 Mirochnitchenko, O. and Inouye, M. (1996) J. Immunol. **156**, 1578–1586
32 Huang, T. T., Yasunami, M., Carlson, E. J., Gillespie, A. M., Reaume, A. G., Hoffman, E. K., Chan, P. H., Scott, R. W. and Epstein, C. J. (1997) Arch. Biochem. Biophys. **344**, 424–432
33 Hohmeier, H. E., Thigpen, A., Tran, V. V., Davis, R. and Newgard, C. B. (1998) J. Clin. Invest. **101**, 1811–1820
34 Lipton, S. A., Choi, Y. B., Pan, Z. H., Lei, S. Z., Chen, H. S., Sucher, N. J., Loscalzo, J., Singel, D. J. and Stamler, J. S. (1993) Nature (London) **364**, 626–632
35 Lamarque, D. and Whittle, B. J. (1995) Br. J. Pharmacol. **116**, 1843–1848
36 Szabo, C., Day, B. J. and Salzman, A. L. (1996) FEBS Lett. **381**, 82–86

37 Pfeiffer, S., Schrammel, A., Koesling, D., Schmidt, K. and Mayer, B. (1998) Mol. Pharmacol. **53**, 795–800
38 Murphy, M. E. and Sies, H. (1991) Proc. Natl. Acad. Sci. U.S.A. **88**, 10860–10864
39 Poderoso, J. J., Carreras, M. C., Lisdero, C., Riobo, N., Schopfer, F. and Boveris, A. (1996) Arch. Biochem. Biophys. **328**, 85–92
40 Yamakura, F., Taka, H., Fujimura, T. and Murayama, K. (1998) J. Biol. Chem. **273**, 14085–14089
41 Szabó, C. and Salzman, A. L. (1995) Biochem. Biophys. Res. Commun. **209**, 739–743
42 Hooper, D. C., Spitsin, S., Kean, R. B., Champion, J. M., Dickson, G. M., Chaudhry, I. and Koprowski, H. (1998) Proc. Natl. Acad. Sci. U.S.A. **95**, 675–680
43 Kane, D. J., Sarafian, T. A., Anton, R., Hahn, H., Gralla, E. B., Valentine, J. S., Örd, T. and Bredesen, D. E. (1993) Science **262**, 1274–1277
44 Mehlen, P., Kretz-Remy, C., Préville, X. and Arrigo, A. P. (1996) EMBO J. **15**, 2695–2706
45 Brockhaus, F. and Brüne, B. (1998) Exp. Cell. Res. **238**, 33–41
46 Bredt, D. S. and Snyder, S. H. (1994) Annu. Rev. Biochem. **63**, 175–195
47 Kinscherf, R., Claus, R., Wagner, M., Gehrke, C., Kamencic, H., Hou, D., Nauen, O., Schmiedt, W., Kovacs, G., Pill, J., Metz, J. and Deigner, H. P. (1998) FASEB J. **12**, 461–467
48 Cho, G., Kang, S., Seo, S. J., Kim, Y. and Jung, G. H. (1997) Biochem. Mol. Biol. Int. **42**, 949–956

Received 30 June 1998/4 November 1998; accepted 8 December 1998